ISSN 1846-6168 (Print), ISSN 1848-5588 (Online)
https://doi.org/10.31803/tg-20230417145110

Original scientific paper
Received: 2023-04-17, Accepted: 2023-04-21

Artificial Neural Network System for Predicting Cutting Forces in Helical-End Milling of Laser-Deposited Metal Materials

Uroš Župerl*, Miha Kovačič

Abstract: When machining difficult-to-cut metal materials often used to make sheet metal forming tools, excessive cutting force jumps often break the cutting edge. Therefore, this research developed a system of three neural network models to accurately predict the maximal cutting forces on the cutting edge in helical end milling of layered metal material. The model considers the different machinability of individual layers of a multilayer metal material. Comparing the neural force system with a linear regression model and experimental data shows that the system accurately predicts the cutting force when milling layered metal materials for a combination of specific cutting parameters. The predicted values of the cutting forces agree well with the measured values. The maximum error of the predicted cutting forces is 5.85% for all performed comparative tests. The obtained model accuracy is 98.65%.

Keywords: cutting forces; helical end milling; layered metal material; linear regression; neural model

1 INTRODUCTION

Multilayer metal materials are increasingly used in tool shops to produce modern metal-forming tools for the automotive industry. The properties of individual layers of such material are determined according to the given requirements. There are quite a few processes available for producing such materials, the most widespread of which is the LENS (laser-engineered net shaping) process [1]. In this process, the workpiece is made layer by layer. If individual layers are produced with different process parameters, the machinability of these layers is variable. The machinability of such materials represents a significant challenge for the metal processing industry. The mechanical processing of these inhomogeneous materials is highly demanding and leads to frequent damage to the tool's cutting edges and excessive tool wear. Tool breakage and wear can be directly related to cutting forces. Knowledge of the maximum cutting forces on the tool enables the precise selection of cutting parameters, thereby reducing processing errors and increasing the tool's life.

Advanced machine tools enable cutting force control and adjust the parameters to current cutting conditions. Knowing the maximum cutting forces and advanced control of the cutting forces makes it possible to efficiently machine even difficult-to-cut non-homogeneous multi-layered materials.

In the literature, it is possible to find some research on processing multi-directional layered metal materials. The most common is research on the machinability of hard-to-machine nickel-based alloys [2, 3], titanium alloys [4] and laminates [5]. An overview of difficult-to-machine alloys, which are most often used in the aerospace, nuclear and medical industries, was given by researchers in work [6]. LI et al. [7] presented a literature review on the machinability of additively manufactured titanium alloys.

Altiparmak et al. [8] studied the machinability of high-strength aluminium alloys manufactured using additive technologies.

The researchers [9] studied the mechanism of chip formation in cutting laser-deposited materials: They found it to be complex and not the same as in the processing of homogeneous materials, where mostly form chips are formed.

Many models of cutting forces for end-milling can be found in the literature. Most mechanistic models [10] have proven robust, simple and effective. More sophisticated models consider radial cutter runout [11], tool deflection [12], system dynamics, cutter contact area [13], indentation of the cutting edge into the work material [14], dynamic chip thickness [15], chip forming and friction forces [16] and radius of curvature for sculptured surface machining [17]. In all these models, the cutting forces are calculated as the product of the uncut chip thickness and the specific cutting forces [18]. In mechanistic models, the helical end-mill is divided in the axial direction into differentially thin elements. The product of the specific cutting force and the uncut chip cross-section area determines the differential force on each differential element. By integrating the differential cutting forces over the entire height of the tool's cutting edge, which is in contact with the workpiece, the total cutting force on the tool is then determined. A few studies have been published that deal with the modeling of cutting forces in helical-end milling composites [19, 20, 21]. Models have been created that consider a unique method of determining the specific cutting force from orthogonal (cutting data) cutting data, the geometry of the chips, the geometry of the tool and the cutting parameters [22, 23]. The research [24] on creating a model of cutting forces for milling carbon fibre-reinforced polymer (CFRP) composites is essential. This model calculated the specific cutting forces by considering the current chip thickness and cutting speed. The main challenge in producing these models is the labor-intensive acquisition of specific cutting forces for shape cutting. Obtaining specific cutting forces for different combinations of tools and workpieces represents a great challenge, as it requires a lot of experimental and analytical work. This is particularly difficult in the case of multi-layer materials with different

machinability of individual layers. Therefore, in this research, we developed a methodology to automatically determine cutting forces for helical-end mills. The procedure is based on a short-term measure of cutting forces under certain cutting conditions. Immediately after the measurement, the obtained data and the corresponding cutting conditions are autonomously transmitted to the artificial intelligence. An artificial neural network automatically generates a model of the cutting forces in a few seconds. This type of modeling is fully automated and does not require human intervention. Obtaining specific cutting forces is not necessary. Many models of cutting forces based on neural networks have been published [25-27] and have been shown to be very accurate in prediction.

The article is organized as follows. Chapter 2 presents the modeling of cutting forces and helical-end milling of layered laser deposited materials. In chapter 3, three artificial neural network models for predicting the cutter's maximum cutting forces in the helical end-milling of laser-deposited metal materials are presented in detail. In chapter 4, the linear regression model of cutting forces is presented. In the next chapter, the results of the models are analyzed. Chapter 6 describes the experimental procedure of data acquisition. Section 7 gives the concluding remarks.

2 MODELING OF CUTTING FORCES IN HELICAL-END MILLING OF LAYERED LASER DEPOSITED MATERIALS

The mechanistic technique that divides the cutter in the axial axis into thin, small elements is often used to model cutting forces in helical-end milling (Fig. 1).

The differential cutting force on the thin element of the cutting tool is determined based on the cutting tool geometry by multiplying the cross-section of the chip and the specific cutting force for that part of the layered material that is in contact with the thin element of the tool. The total cutting force is determined by adding all differential cutting forces on all thin tool elements in contact with the workpiece. To calculate the differential cutting forces on a thin tool element, verified equations are available in the literature, and the calculation does not cause problems. A significant challenge is the experimental determination of specific cutting forces for each layer of a multilayer laser-deposited material. The specific cutting force for a material layer is determined as the ratio between the experimentally determined current component of the cutting force and the calculated cross-section of the chip. This process is time-consuming, demanding and labour-intensive.

Therefore, in this research, we developed a methodology to quickly determine cutting forces for helical-end mills. The procedure is based on a short-term measure of cutting forces under certain cutting conditions. Immediately after the measurement, the obtained data and the corresponding cutting conditions are autonomously transmitted to the artificial intelligence. An artificial neural network automatically generates a model of the cutting forces in 2-3 seconds. With further measurements, the already developed neural network model is supplemented with new data. This type of modeling is fully automated and does not require human intervention. Several artificial neural network architectures have been tested to achieve rapid model generation. Three of the most effective neural network architectures are presented, best adapted to modeling cutting forces in helical-end milling.

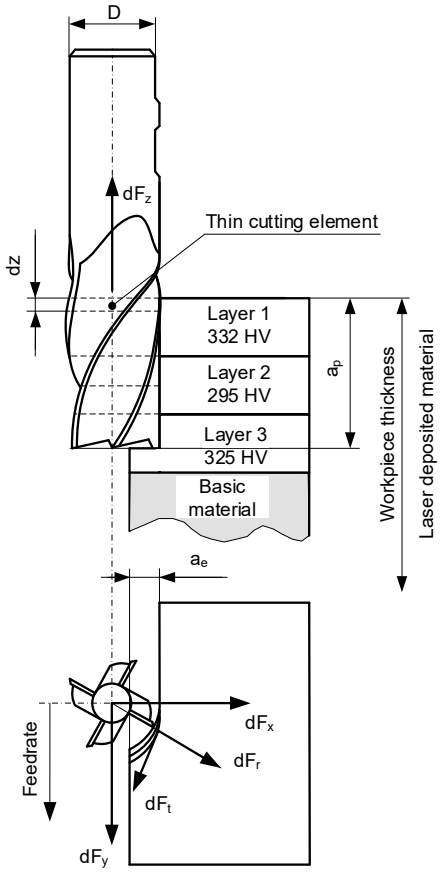

Figure 1 Cutting forces on a thin cutting disc in helical end milling of layered material.

3 ARTIFICIAL NEURAL NETWORK MODELS

The purpose of this research is to create a system of three artificial neural networks for predicting the maximum cutting forces on the cutter in the process of helical end-milling of laser-deposited metal materials. This chapter presents the architectures of three different neural networks adapted to the problem of predicting cutting forces based on a tiny sample of data for learning and testing.

Three different neural network architectures were constructed. The cutting parameters were entered into the neural networks as input data. The output data (result) was the maximum cutting force. Maximum cutting force is the maximum cutting force that occurs during one cutter rotation.

The popular multilayer feedforward neural network architecture was used for cutting force modeling. The neural networks were created in the Matlab software package using the nntraintool tool.

The neural model for predicting cutting forces is built in 4 steps. In the first step, the data for learning and validating

the neural model of cutting forces were obtained in the machining experiment.

This step made 36 measurements of the maximum cutting force on the milling cutter. Among the 36 measurements, 27 measurements were used to learn the neural networks, and 9 measurements were used to test the neural network's performance.

Tab. 1 shows 27 datasets for learning and 9 testing datasets. The test datasets are highlighted. The Tab. 1 consists of 5 columns.

The first column contains the serial number of the experiment - measurements, the second to fourth columns have the input data for the ANN, and the last column represents the output vector with the target value, i.e. the value of the maximal measured cutting force.

This step transferred the learning and testing data sets to the ANN.

Table 1 Datasets for model learning and testing.

Measurement No.:	Spindle speed (min^{-1})	Feed rate (mm/min)	a_p (mm)	Cutting force (N)
1	2000	390	0.27	174.63
2	2500	390	0.27	166.75
3	3000	390	0.27	149.38
4	3000	960	0.27	153.32
5	2500	960	0.27	186.45
6	2000	960	0.27	198.77
7	2000	2700	0.27	200.08
8	2500	2700	0.27	196.55
9	3000	2700	0.27	191.90
10	3000	6000	0.27	207.15
11	2500	6000	0.27	213.82
12	2000	6000	0.27	218.46
13	2000	390	0.72	180.89
14	2500	390	0.72	174.83
15	3000	390	0.72	151.20
16	3000	960	0.72	156.35
17	2500	960	0.72	188.77
18	2000	960	0.72	197.96
19	2000	2700	0.72	209.37
20	2500	2700	0.72	196.14
21	3000	2700	0.72	183.21
22	3000	6000	0.72	198.16
23	2500	6000	0.72	213.21
24	2000	6000	0.72	218.97
25	2000	390	1.40	188.16
26	2500	390	1.40	183.01
27	3000	390	1.40	159.68
28	3000	960	1.40	163.72
29	2500	960	1.40	191.90
30	2000	960	1.40	196.45
31	2000	2700	1.40	209.68
32	2500	2700	1.40	196.65
33	3000	2700	1.40	177.76
34	3000	6000	1.40	183.11
35	2500	6000	1.40	207.05
36	2000	6000	1.40	212.50

In step 2, the architecture of the neural network is defined.

Learning algorithms, activation functions, error for evaluating the predictive model's performance and learning parameters are defined.

The learning phase of the neural network is performed in step 3.

During the learning phase, the weights on the synapses between the neurons are set. In this way, the internal structure of the neural network adapts to the learning data and provides the correct predicted results according to the input features.

In the fourth step, the neural network model is completed and ready for use; prediction of cutting forces.

All three designed ANN architectures have three neurons in the input level: spindle speed n, feed rate f and axial depth of cut AD.

The radial depth of cut R_D was constant in all machining experiments.

The output from the ANN is the maximum cutting force generated in one tool rotation, so only one neuron is needed at the output level.

The first constructed neural network (ANN1) has one hidden level with three neurons. In one hidden layer, Sigmoid activation function is used. The scaled conjugate gradient learning algorithm (trsinscg) is used.

The performance of the learned network was determined based on Mean Squared Error (mse). The detailed architecture of the designed ANN1 with algorithm parameters and learning progress are shown in Fig. 2.

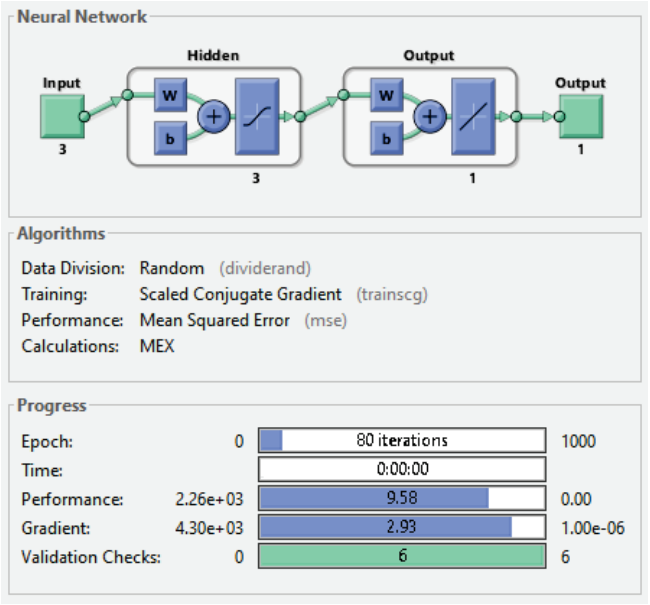

Figure 2 The detailed architecture of the designed ANN1 with algorithm parameters and learning progress.

Fig. 3 shows the learning flow of ANN1. The stopping condition on the validation set was triggered at the 72nd iteration when the MSE error value reached a minimum value of 4.2. At 72 iterations, ANN1 is the best learned and most accurately predicts cutting forces.

The gradient of the neural network is associated with the green curve. Learning stops when a stop rule is triggered, i.e. when the global minimum is reached (in the following six iterations the learning of the neural network does not improve).

The program then displays the learning results of the neural network.

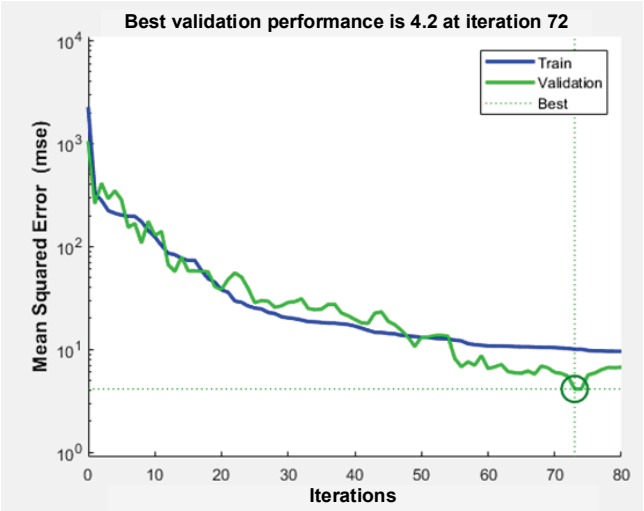

Figure 3 Learning and validation curves of the ANN1

Fig. 4 shows the match between the values of predicted (blue line) and measured cutting forces marked with circles. ANN1 compares the predicted cutting force values with the measured cutting force values. The dashed line (diagonal of the square) shows the ideal relationship between the measurements and the predicted values of ANN1. In Fig. 4, the predicted values with the dashed line almost overlap, this is shown by the value of $R = 0.98517$.

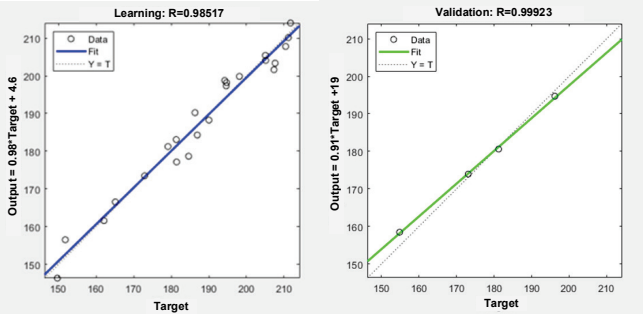

Figure 4. Learning and validation results of the ANN1 neural network.

Out of 27 measurements, four not used in the learning process were randomly selected for validation (Fig. 4). The linear regression results between the measured and predicted cutting forces is given with a value of $R = 0.99923$.

The second constructed neural network (ANN2) has one hidden level with six neurons. In the hidden layer, Sigmoid activation function is used. The Levenberg-Marquardt learning algorithm (trainlm) is used. The performance of the learned network was determined based on Mean Squared Error (mse). The detailed architecture of the designed ANN2 with algorithm parameters and learning progress are shown in Fig. 5.

Fig. 6 shows the learning flow of ANN2. The stopping condition on the validation set was triggered at iteration 12 when the MSE error value reached a minimum value of 17.4. The gradient of the ANN2 reached a global minimum at the sixth iteration. ANN2 learned with six iterations predicts cutting forces most accurately. The gradient of the neural network is associated with the green curve.

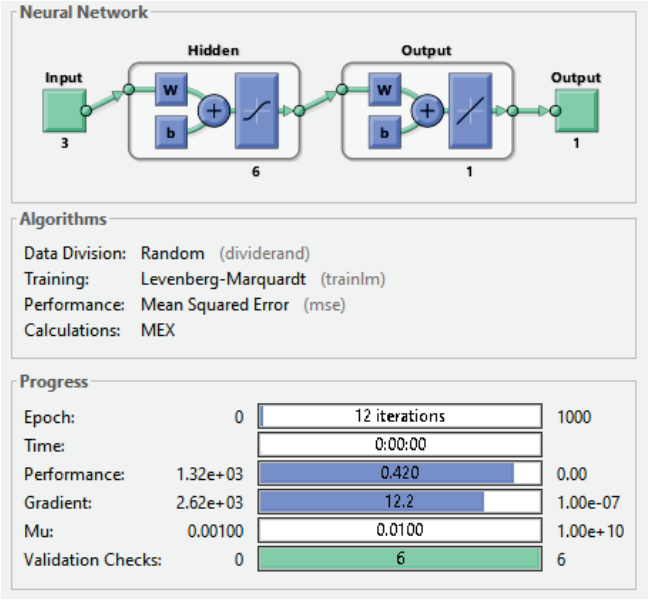

Figure 5 The detailed architecture of the designed ANN2 with algorithm parameters and learning progress.

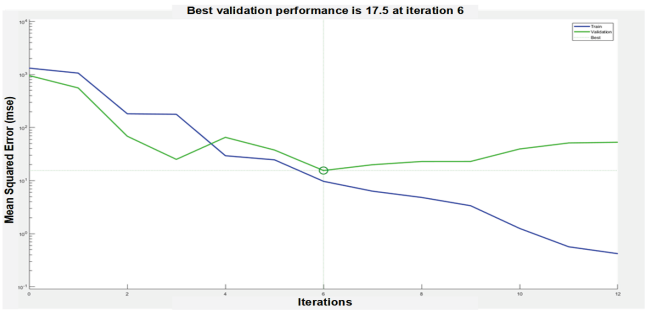

Figure 6 Learning and validation curves of the ANN2

Compared to ANN1, the match between predicted values and measured cutting forces was similar, with neural network learning achieving a ratio of $R = 0.974113$.

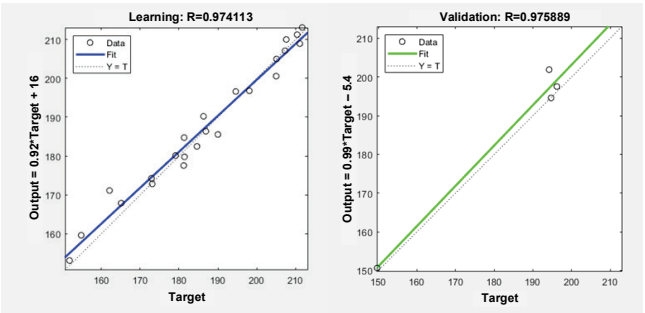

Figure 7. Learning and validation results of the ANN2 neural network.

In the validation, the linear regression results between the measured and predicted cutting forces are given with a value of $R = 0.975889$, which is similar to the results of ANN1 (Fig. 7).

The third constructed neural network (ANN3) has one hidden level with seven neurons. In hidden layer, Sigmoid activation function is used. The BFGS Quasi-Newton learning algorithm (trainbfg) is used. The performance of the

learned network was determined based on Mean Squared Error (mse). The detailed architecture of the designed ANN3 with algorithm parameters and learning progress are shown in Fig. 8.

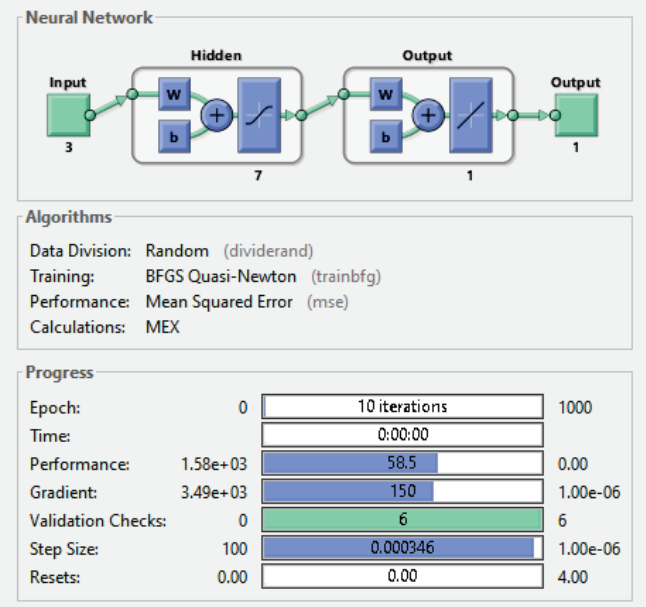

Figure 8 The detailed architecture of the designed ANN3 with algorithm parameters and learning progress.

Fig. 9 shows the learning diagram of ANN3.

The stopping condition in the validation set was triggered at the iteration 14 when the MSE error value reached a value of 37.31.

The gradient of the ANN3 reached a global minimum at 9th and 12th iterations. In the 14th iteration, the lowest MSE value was reached.

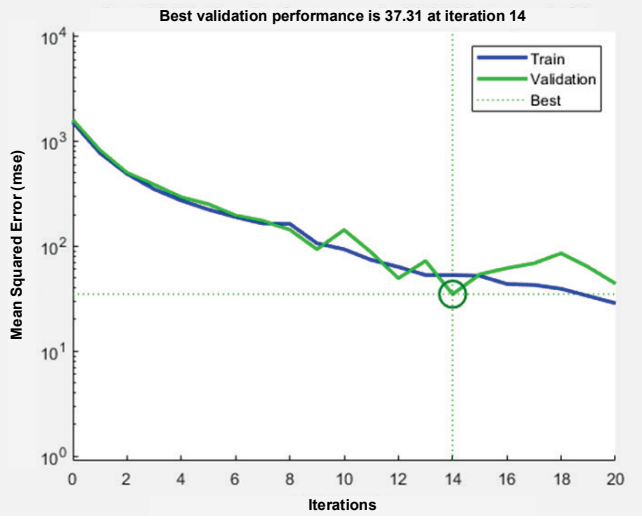

Figure 9 Learning and validation curves of the ANN3

The match between the predicted and measured values of the cutting forces during learning is given by the parameter R = 0.9359, which is the worst result of all the constructed neural networks (Fig. 10).

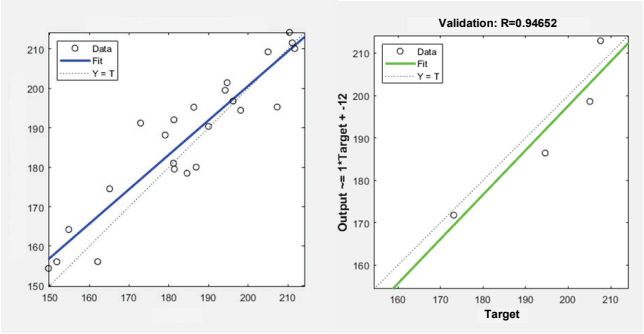

Figure 10 Learning and validation results of the ANN2 neural network.

The results of the linear regression between the measured and predicted cutting forces are given with a value of R = 0.94652, which is also the worst of all three neural networks.

4 A LINEAR REGRESSION MODEL FOR PREDICTING CUTTING FORCES

A simple linear regression model was constructed to predict cutting force as a function of cutting parameters. The designed linear regression model predicts with 90.3% accuracy.

A linear regression model for predicting cutting forces is given by:

$$F = +246.01 - 0.02901 \cdot spindle\ speed + 0.37101 \cdot feed\ rate - 0.065991 \cdot A_{\mathrm{D}} \quad (1)$$

The results of the linear regression model compared to the measured values are given in Tab. 2.

Table 2 Comparison of predicted and measured cutting forces.

No.:	Spindle speed (min^{-1})	Feed rate (mm/min)	a_p (mm)	Cutting force (N)	Predicted cutting force (N)
3	3000	390	0.27	149.4	164.84
6	2000	960	0.27	198.8	204.18
9	3000	2700	0.27	191.9	195.98
12	2000	6000	0.27	218.5	278.33
18	2000	960	0.72	198.0	203.84
24	2000	6000	0.72	219.0	277.99
27	3000	390	1.40	159.7	163.99
30	2000	960	1.40	196.4	203.33
33	3000	2700	1.40	177.8	195.13

5 RESULTS AND DISCUSSION

The research aimed to create a system of three neural network models for predicting cutting forces and to compare the results of the models with the measured values of the cutting forces and with the results of the linear regression model.

All three artificial neural networks and the linear regression model were trained with data from 27 measurements and tested with data from 9 measurements. The obtained results from neural networks and linear regression models, together with the measured cutting forces, are shown in Tab. 3 and Fig. 11.

Table 3 Comparison of model results with measurements.

No.:	Measured cutting force (N)	Cutting force (N) ANN1	ANN2	ANN3	Linear regression model
3	149.4	144.0	149.5	160.8	164.84
6	198.8	186.1	187.2	184.1	204.18
9	191.9	182.1	184.7	181.3	195.98
12	218.5	216.1	213.9	222.3	278.33
18	198.0	191.9	191.9	193.8	203.84
24	219.0	212.8	215.3	220.1	277.99
27	159.7	154.3	162.8	158.4	163.99
30	196.4	198.2	201.0	199.6	203.33
33	177.8	175.2	175.2	182.0	195.13

Table 4 Deviation of predicted values from measurements.

No.:	Measured cutting force (N)	Prediction error (%) ANN1	ANN2	ANN3	Linear regression model
3	149.4	3.60	–0.07	–7.71	–10.39
6	198.8	6.38	5.85	7.43	–2.73
9	191.9	5.15	3.75	5.54	–2.13
12	218.5	1.09	2.11	–1.78	27.54
18	198.0	3.07	3.10	2.12	2.98
24	219.0	2.84	1.68	–0.50	27.08
27	159.7	3.38	–1.93	0.83	2.70
30	196.4	–0.88	–2.33	–1.64	3.52
33	177.8	1.46	1.46	–2.39	9.81
	Model accuracy	97.13	98.65	97.21	92,52

The predicted cutting force values of the three neural networks are very similar to each other, but due to the small number of samples, the linear regression model predicted the results worse than the neural networks.

Fig. 12 and Tab. 4 show the average error of the predicted cutting force values compared to the measured cutting force.

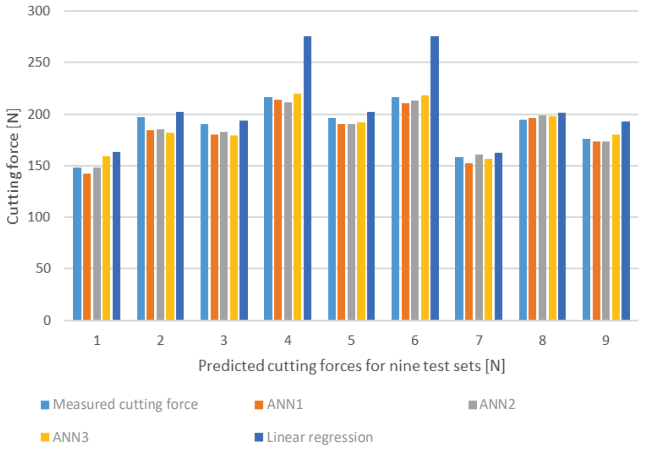

Figure 11 Comparison of model results with measurements

The results show that the neural network models are more accurate than the linear regression model and that the average error of the predicted cutting force is smaller than the model made by linear regression. Among all the neural networks, the ANN2 neural network showed the best results, with a maximum deviation of 5.85%.

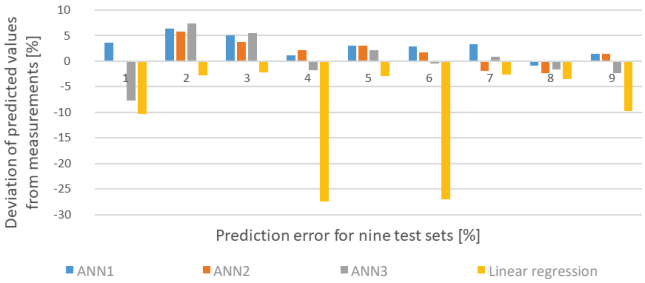

Figure 12 Deviation of predicted values from measurements

6 EXPERIMENTAL TESTS TO OBTAIN DATA

To create 3 neural networks and verify the predictive capabilities of the models, machining experiments were performed at the Heler BEA 02 machining centre. For the helical end milling process, carbide milling cutters with a diameter of 9 mm with two flutes, 28.1° helix angle and 3.80° rake angle were used. The tool material is sintered tungsten carbide with TiAlN coating and a hardness of 1800 HV.

The workpiece was produced on the Optomec LENS 850-R machine. The primary material of the workpiece is steel 20MnCr5. Three thick layers of stainless steel (316L) are applied to the 20MnCr5 steel base. The deposited layers have different properties (Fig. 1). The layers are made with 38% overlap. The thicknesses and harnesses of the individual layers are shown in Fig. 1 and range from 295 HV to 332 HV.

The maximum cutting forces that occur during one cutter rotation were measured with a Kistler 9257A piezoelectric dynamometer with a natural frequency of 3.5 kHz. A Dual Mode amplifier (NI 9215A) is used to amplify the charge. A low pass filter of 1.2 kHz cut-off frequency is used for filtering. The conversion of the charge into a voltage from 0-10V was performed by a data acquisition card manufactured by National Instruments. LabVIEW software was used to develop the measurement application. Each measurement was repeated three times.

Measurements were made at three milling depths: 0.27 mm, 0.72 mm and 1.40 mm. For each milling depth, 12 different measurements were made, which depended on feed and cutting speed. Three different tool frequencies were used: 2000, 2500 and 3000 rpm, and four different feed rates: 390 mm/min, 960 mm/min, 2700 mm/min and 6000 mm/min. All 36 measurements are shown in Tab. 1. Nine measurements were used to verify the manufactured models.

Fig. 1 schematically shows a machining experiment with a tool and a workpiece for the development and verification of models of cutting forces.

7 CONCLUSIONS

This article presents a system of three artificial neural networks models for accurate prediction of the maximal cutting forces on cutting edge of a cutter in helical end milling of layered metal material with different machinability of individual layers. The workpiece material is classified as a difficult-to-machine material. Artificial neural network models were developed in Matlab software.

The goal of the research is to replace the long-term analytical determination of maximum tool loads when machining materials with layers of different machinability by automatically creating models based on artificial intelligence from the smallest amount of experimental data.

The results provide a comparison between predicted cutting forces using linear regression and neural networks models and experimentally obtained values. It turns out that all three neural network models (ANN1, ANN2, ANN3) of cutting forces have an average error of less than 6.5% and are more accurate than the linear regression model. The maximal cutting forces predicted by the neural models are in good agreement with the experimentally obtained ones.

The second neural network (ANN2) proved to be the most accurate of the three with the largest deviation of 5.85% from all measurements and 98.65% model accuracy.

8 REFERENCES

[1] Mahmoud, E. R. I. (2015). Characterizations of 304 stainless steel laser cladded with titanium carbide particles. *Advances in Production Engineering & Management, 10*(6), 115-124. https://doi.org/10.14743/apem2015.3.196

[2] Zhang, S., Li, J. F., & Wang, Y. W. (2012). Tool life and cutting forces in end milling Inconel 718 under dry and minimum quantity cooling lubrication cutting conditions. *Journal of Cleaner Production*, *32*, 81-87. https://doi.org/10.1016/j.jclepro.2012.03.014

[3] Tabernero, I., Lamikiz, A., Martínez, S., Ukar, E., & Figueras, J. (2011). Evaluation of the mechanical properties of Inconel 718 components built by laser cladding. I*nternational Journal of Machine Tools and Manufacture, 51*(6), 465-470. https://doi.org/10.1016/j.ijmachtools.2011.02.003

[4] Jia, Z. Y., Ge, J., Ma, J. W., Gao, Y. Y., & Liu, Z. (2016). A new cutting force prediction method in ball-end milling based on material properties for difficult-to-machine materials. *The International Journal of Advanced Manufacturing Technology, 86*(9-12), 2807-2822. https://doi.org/10.1007/s00170-016-8351-8

[5] Dandekar, C. R., & Shin, Y. C. (2012). Modeling of machining of composite materials: A review. *International Journal of Machine tools and manufacture, 57*, 102-121. https://doi.org/10.1016/j.ijmachtools.2012.01.006

[6] Shokrani, A., Dhokia, V., Newman, S.T. (2012). Environmentally conscious machining of difficult-to-machine materials with regard to cutting fluids. *International Journal of Machine Tools and Manufacture, 57*, 83-101. https://doi.org/10.1016/j.ijmachtools.2012.02.002

[7] Li, G., Chandra, S., Rashid, R. A. R., Palanisamy, S., & Ding, S. (2022). Machinability of additively manufactured titanium alloys: A comprehensive review. *Journal of Manufacturing Processes, 75,* 72-99. https://doi.org/10.1016/j.jmapro.2022.01.007

[8] Altıparmak, S. C., Yardley, V. A., Shi, Z., & Lin, J. (2021). Challenges in additive manufacturing of high-strength aluminium alloys and current developments in hybrid additive manufacturing. *International Journal of Lightweight Materials and Manufacture, 4*(2), 246-261. https://doi.org/10.1016/j.ijlmm.2020.12.004

[9] M'Saoubi, R., Axinte, D., Soo, S. L., Nobel, C., Attia, H., Kappmeyer, G., Engin, S., & Sim, W. M. (2015). High performance cutting of advanced aerospace alloys and composite materials. *CIRP Annals-Manufacturing Technology, 64*(2), 557-580. https://doi.org/10.1016/j.cirp.2015.05.002

[10] Song, G., Sui, S., & Tang, L. (2015). Precision prediction of cutting force in oblique cutting operation. *The International Journal of Advanced Manufacturing Technology, 81*(1-4), 553-562. https://doi.org/10.1007/s00170-015-7206-z

[11] Sun, Y., & Guo, Q. (2011). Numerical simulation and prediction of cutting forces in five-axis milling processes with cutter run-out. *International Journal of Machine Tools and Manufacture, 51*(10-11), 806-815. https://doi.org/10.1016/j.ijmachtools.2011.07.003

[12] Omar, O. E. E. K., El-Wardany, T., Ng, E., & Elbestawi, M. A. (2007). An improved cutting force and surface topography prediction model in end milling. *International Journal of Machine Tools and Manufacture, 47*(7-8), 1263-1275. https://doi.org/10.1016/j.ijmachtools.2006.08.021

[13] Wei, Z. C., Wang, M. J., Zhu, J. N., & Gu, L. Y. (2011). Cutting force prediction in ball end milling of sculptured surface with Z-level contouring tool path. *International Journal of Machine Tools and Manufacture, 51*(5), 428-432. https://doi.org/10.1016/j.ijmachtools.2011.01.011

[14] Tuysuz, O., Altintas, Y., & Feng, H. Y. (2013). Prediction of cutting forces in three and five-axis ball-end milling with tool indentation effect. *International Journal of Machine Tools and Manufacture, 66,* 66-81. https://doi.org/10.1016/j.ijmachtools.2012.12.002

[15] Qu, S., Zhao, J., Wang, T., & Tian, F. (2015). Improved method to predict cutting force in end milling considering cutting process dynamics. *The International Journal of Advanced Manufacturing Technology, 78*(9-12), 1501-1510. https://doi.org/10.1007/s00170-014-6731-5

[16] Du, J., Li, J., Yao, Y., & Hao, Z. (2014). Prediction of cutting forces in mill-grinding SiCp/Al composites. *Materials and Manufacturing Processes, 29*(3), 314-320. https://doi.org/10.1080/10426914.2013.864402

[17] Cao, Q., Zhao, J., Li, Y., & Zhu, L. (2013). The effects of cutter eccentricity on the cutting force in the ball-end finish milling. *The International Journal of Advanced Manufacturing Technology, 69*(9-12), 2843-2849. https://doi.org/10.1007/s00170-013-5205-5

[18] Li, Y., Yang, Z. J., Chen, C., Song, Y. X., Zhang, J. J., & Du, D. W. (2018). An integral algorithm for instantaneous uncut chip thickness measuring in the milling process. *Advances in Production Engineering & Management, 13*(3), 297-306. https://doi.org/10.14743/apem2018.3.291

[19] Denkena, B., Boehnke, D., & Dege, J. H. (2008). Helical milling of CFRP–titanium layer compounds. *CIRP Journal of manufacturing Science and Technology, 1*(2), 64-69. https://doi.org/10.1016/j.cirpj.2008.09.009

[20] Karpat, Y., & Polat, N. (2013). Mechanistic force modeling for milling of carbon fiber reinforced polymers with double helix tools. *CIRP Annals, 62*(1), 95-98. https://doi.org/10.1016/j.cirp.2013.03.105

[21] Kalla, D., Sheikh-Ahmad, J., & Twomey, J. (2010). Prediction of cutting forces in helical end milling fiber reinforced polymers. International Journal of Machine *Tools and Manufacture, 50*(10), 882-891. https://doi.org/10.1016/j.ijmachtools.2010.06.005

[22] Budak, E., Altintas, Y., & Armarego, E. J. A. (1996). Prediction of milling force coefficients from orthogonal cutting data. *Journal of Manufacturing Science and Engineering, 118*(2), 216-224. https://doi.org/10.1115/1.2831014

[23] Gradišek, J., Kalveram, M., & Weinert, K. (2004). Mechanistic identification of specific force coefficients for a general end mill. *International Journal of Machine Tools and Manufacture, 44*(4), 401-414. https://doi.org/10.1016/j.ijmachtools.2003.10.001

[24] He, Y., Qing, H., Zhang, S., Wang, D., & Zhu, S. (2017). The cutting force and defect analysis in milling of carbon fiber-reinforced polymer (CFRP) composite. *The International Journal of Advanced Manufacturing Technology, 93*, 1829-1842. https://doi.org/10.1007/s00170-017-0613-6

[25] El-Mounayri, H., Briceno, J. F., & Gadallah, M. (2010). A new artificial neural network approach to modeling ball-end milling. *The International Journal of Advanced Manufacturing Technology, 47*(5-8). https://doi.org/10.1007/s00170-009-2217-2

[26] Al-Zubaidi, S., Ghani, J. A., & Haron, C. H. C. (2011). Application of ANN in milling process: a review. *Modelling and Simulation in Engineering, 9,* 1-7. https://doi.org/10.1155/2011/696275

[27] Kalla, D., Sheikh-Ahmad, J., & Twomey, J. (2010). Prediction of cutting forces in helical end milling fiber reinforced polymers. *International Journal of Machine Tools and Manufacture, 50*(10), 882-891. https://doi.org/10.1016/j.ijmachtools.2010.06.005

Authors' contacts:

Uroš Župerl, Assoc. Prof.
(Corresponding author)
University of Maribor, Faculty of Mechanical Engineering,
Smetanova ulica 17, 2000 Maribor, Slovenia
+38622207621, uros.zuperl@um.si

Miha Kovačič, Assoc. Prof.
ŠTORE STEEL. d.o.o., Štore
Železarska cesta 3, 3220 Štore, Slovenija
University of Ljubljana, Faculty of Mechanical Engineering,
Aškerčeva cesta 6, 1000 Ljubljana, Slovenia
College of Industrial Engineering Celje, Celje
Mariborska cesta 2, 3000 Celje, Slovenia
+386 (0)3 7805 262, miha.kovacic@store-steel.si